



# The resonant behavior in the oscillator with double fractional-order damping under the action of nonlinear multiplicative noise



Yan Tian <sup>a,\*</sup>, Lin-Feng Zhong <sup>b,c,d,\*\*</sup>, Gui-Tian He <sup>a</sup>, Tao Yu <sup>e</sup>, Mao-Kang Luo <sup>e</sup>,  
H. Eugene Stanley <sup>d</sup>

<sup>a</sup> School of science, Southwest Petroleum University, ChengDu 610500, PR China

<sup>b</sup> Web Sciences center, University of Electronic Science and Technology of China, Chengdu 610054, PR China

<sup>c</sup> Big data research center, University of Electronic Science and Technology of China, Chengdu 610054, PR China

<sup>d</sup> Center for Polymer Studies and Department of Physics, Boston, MA 02215, USA

<sup>e</sup> College of Mathematics, Sichuan University, ChengDu 610064, PR China

## HIGHLIGHTS

- SR is studied in the system with double fractional-order damping and nonlinear noise.
- The resonance is diverse when there is nonlinear noise.
- The order of the fractional-order damping strongly impacts resonant intensity.
- The impact of external and intrinsic damping on resonant intensity is the opposite.

## ARTICLE INFO

### Article history:

Received 26 March 2017

Received in revised form 13 June 2017

Available online 1 September 2017

### Keywords:

Nonlinear noise

The fractional-order external damping

The fractional-order intrinsic damping

Stochastic resonance

## ABSTRACT

We study stochastic resonance (SR) in an oscillator with nonlinear noise, fractional-order external damping, and fractional-order intrinsic damping. Using a moment equation, we derive the exact analytical expression of the output amplitude and find that fluctuations in the output amplitude are non-monotonic. Using numerical simulations we verify the accuracy of this analytical result. We find (i) that nonlinear noise plays a key role in system behavior and that the resonance of the output amplitude is diverse when there is nonlinear noise, (ii) that the order of the fractional-order damping strongly impacts resonant intensity and that the impact on resonant intensity of fractional-order external damping is opposite that of fractional-order intrinsic damping, and (iii) that the evolution of the output amplitude versus the frequency of the external periodic force exhibits three behaviors: a resonance with one peak, a resonance with one peak and one valley, and a resonance with one valley.

© 2017 Elsevier B.V. All rights reserved.

\* Corresponding author.

\*\* Correspondence to: Web Sciences center, University of Electronic Science and Technology of China, Chengdu 610054, PR China.  
E-mail addresses: [yantiancd@126.com](mailto:yantiancd@126.com) (Y. Tian), [googlezlf@163.com](mailto:googlezlf@163.com) (L.-F. Zhong).

## 1. Introduction

The harmonic oscillator is a simple model for different phenomena in nature, and it is the most widely used in physics. A forced harmonic oscillator can be defined as

$$m\ddot{x}(t) + \gamma\dot{x}(t) + \omega^2x(t) = f(t), \quad (1)$$

where  $x(t)$  is the displacement of the oscillator at time  $t$ ,  $m$  the mass of the oscillator,  $\gamma$  the friction constant,  $\omega^2$  the intrinsic frequency of the system, and  $f(t)$  the external periodic force. The damping term  $\gamma\dot{x}(t)$  is caused by such external influences as friction and is thus designated external damping. This external damping is solely dependent on the current speed and thus can describe such pure viscous media as water.

Because the damping generated by such complex systems as viscoelastic media, magneto-rheological fluids, and amorphous semiconductors is connected to the historical speed, we replace the usual damping term  $\gamma\dot{x}(t)$  with a power-law damping term  $\gamma\mathcal{D}^\beta x(t)$ , ( $0 < \beta \leq 1$ ) [1] and obtain an oscillator with power-law external damping,

$$m\ddot{x}(t) + \gamma\mathcal{D}^\beta x(t) + \omega^2x(t) = f(t), \quad (0 < \beta \leq 1), \quad (2)$$

where  $\mathcal{D}^\beta x(t) = \frac{1}{\Gamma(1-\beta)} \int_0^t (t-\tau)^{-\beta} \dot{x}(\tau) d\tau$ , ( $0 < \beta \leq 1$ ) is the Caputo's fractional derivative of  $x(t)$ ,  $\gamma\mathcal{D}^\beta x(t)$  is the fractional-order external damping, and  $\beta$  is the order of the fractional-order external damping.

An oscillator of viscoelastic materials consumes energy as it oscillates and becomes attenuated. Unlike the external damping generated by external friction, the damping generated by the oscillator itself is intrinsic [2]. To describe intrinsic damping, we replace  $m\ddot{x}(t)$  in Eq. (2) with  $m\mathcal{D}^\alpha x(t)$ , ( $1 < \alpha \leq 2$ ) [2–4] and obtain an oscillator with double fractional-order damping,

$$m\mathcal{D}^\alpha x(t) + \gamma\mathcal{D}^\beta x(t) + \omega^2x(t) = f(t), \quad (0 < \beta \leq 1, 1 < \alpha \leq 2), \quad (3)$$

where  $\mathcal{D}^\rho x(t) = \frac{1}{\Gamma(n-\rho)} \int_0^t (t-\tau)^{n-\rho-1} x^{(n)}(\tau) d\tau$ , ( $n-1 < \rho \leq n$ ),  $m\mathcal{D}^\alpha x(t)$  is the fractional-order intrinsic damping and  $\gamma\mathcal{D}^\beta x(t)$  is the fractional-order external damping.

Systems often experience external fluctuation. Einstein used a noisy oscillator 100 years ago to study Brownian motion. Although noise is often destructive in nature, the SR phenomenon indicates that under certain conditions noise can make a system more coherent [5]. The concept of SR was originally proposed by R. Benzi et al. [6] to explain the periodicity of ice ages on Earth in early 1980s. The conventional SR refers to the phenomenon that the signal to noise ratio (SNR) is non-monotonic with the change of characteristic parameters of noise (such as noise intensity and correlation rate). The SR in a broad sense was introduced by Gitterman [7], which means that the non-monotonic behavior of certain function of output signal (such as moment, autocorrelation function, power spectrum and SNR, etc.) depends on the change of characteristic parameters (such as the frequency and the amplitude of input signal, noise intensity and correlation rate, etc.). There is much literature on the investigation of resonant behavior in oscillators with random frequency, random damping, random phase, and a random mass [8–18]. These models have been applied to many topics, e.g., wave propagation in a random medium [19], turbulent flow on the ocean surface [20], waves in water subjected to turbulent wind [21], open liquid flow [22], dendritic growth [23], and Brownian motion with adhesion [24]. Most of the studies of resonant behavior are usually restricted to the systems with single fractional-order damping, the study of resonant behavior in the oscillators with double fractional-order damping is still at an initial stage. Recently Zhong et al. [17] investigated the resonant behavior in a noisy oscillator,

$$m\mathcal{D}^\alpha x(t) + \gamma\mathcal{D}^\beta x(t) + [\omega^2 + \xi(t)]x(t) = A \sin(\Omega t), \quad (0 < \beta \leq 1, 1 < \alpha \leq 2). \quad (4)$$

Research indicates that the SR phenomenon occurs in oscillators with double fractional-order damping driven by linear noise.

Often chemical and biological solutions are viscoelastic media with molecules that can both collide with Brownian particles and adhere to them. Because the collision of viscoelastic media with Brownian particles is connected to their speed history and molecules' adhesion to them during oscillation causes them to consume energy, we use Eq. (4) to describe Brownian particle movement in viscoelastic media. Note that nonlinear noise is more extensive in real-world systems than linear noise, and that our current understanding of nonlinear noise is too partial for any useful practical application. For example, the fluctuations of external sources affecting pump lasers causes nonlinear fluctuations in their net gain [25]. In Ref. [26] Zhang describes the response of a single-mode laser system to an amplitude modulation signal in the presence of quadratic colored pump noise. Because of the fluctuation of the electronic field intensity and various low-scale thermal noise produced by the quantum effect, the fluctuation noise is usually nonlinear in physical and electronic systems [27]. Thus because the potential  $U(x, t) = \omega^2 x^2(t)/2$  is usually affected by nonlinear noise in Brownian motion, we reformulate Eq. (4) to be

$$m\mathcal{D}^\alpha x(t) + \gamma\mathcal{D}^\beta x(t) + \{\omega^2 + g[\xi(t)]\}x(t) = f(t), \quad (0 < \beta \leq 1, 1 < \alpha \leq 2), \quad (5)$$

where  $g[\xi(t)]$  is the nonlinear function of  $\xi(t)$ . The SR phenomenon is a nonlinear cooperative effect that is jointly induced by external driving, noise and system and is closely related to the noise. Thus the non-linearity of the noise impacts the dynamic behavior of system. Because quadratic noise is the most basic nonlinear noise, we focus our attention on it. There have been prior research. Sagués [28] examined the non-Markovian dynamics of stochastic differential equations with quadratic noise.

Hector [29] found the SR phenomenon in a single stable system driven by quadratic noise. Yu et al. [12] studied resonant behavior in fractional-order Langevin equations with quadratic multiplicative noise.

Using this prior research we examine the resonant behavior in an oscillator with double fractional-order damping driven by quadratic noise. Our goal is to investigate the influence of nonlinear noise and the order of the fractional-order damping on system behavior. Using the fractional Shapiro–Loginov formula [17] and the Laplace transform technique, we obtain the first moment and the amplitude of the output response. We use these results to study resonant behaviors when they are impacted by nonlinear noise, fractional-order external damping, and fractional-order intrinsic damping. To verify the analytical results, we carry out numerical simulations.

### 2. System model

We consider an oscillator with fractional-order external damping and fractional-order intrinsic damping driven by quadratic multiplicative noise and described by the stochastic differential equation

$$\mathcal{D}^\alpha x(t) + \gamma \mathcal{D}^\beta x(t) + [\omega^2 + a_1 \xi(t) + a_2 \xi^2(t)]x(t) = A \cos(\Omega t) \eta(t), \tag{6}$$

$$(0 < \beta \leq 1, 1 < \alpha \leq 2),$$

where external periodic force  $A \cos(\Omega t) \eta(t)$  is a periodically modulated noise,  $a_1 \xi(t) + a_2 \xi^2(t)$  is the quadratic multiplicative noise, and  $a_1$  and  $a_2$  are the linear coefficient and quadratic coefficient of the noise, respectively. Note that  $a_1 \xi(t) + a_2 \xi^2(t)$  is the linear noise for  $a_1 \neq 0, a_2 = 0$  and  $a_1 \xi(t) + a_2 \xi^2(t)$  is the nonlinear noise for  $a_2 \neq 0$ . Here  $\xi(t)$  and  $\eta(t)$  are correlated as

$$\begin{aligned} \langle \xi(t) \rangle &= 0, \langle \xi(t) \xi(s) \rangle = \sigma_\xi \exp(-\lambda_\xi |t - s|); \\ \langle \eta(t) \rangle &= 0, \langle \eta(t) \eta(s) \rangle = \sigma_\eta \exp(-\lambda_\eta |t - s|); \\ \langle \xi(t) \eta(s) \rangle &= \sigma_{\xi\eta} \exp(-\lambda_{\xi\eta} |t - s|). \end{aligned}$$

where  $\sigma_\xi$  and  $\lambda_\xi$  are the noise intensity and correlation rate of  $\xi(t)$ ,  $\sigma_\eta$  and  $\lambda_\eta$  are the noise intensity and correlation rate of  $\eta(t)$ , and  $\sigma_{\xi\eta}$  and  $\lambda_{\xi\eta}$  are the correlation intensity and correlation rate between  $\xi(t)$  and  $\eta(t)$ .

We here assume that  $\xi(t)$  and  $\eta(t)$  are both an asymmetric dichotomous noise (DN).  $\xi(t)$  takes two values  $A_1$  and  $-B_1$  ( $A_1, B_1 > 0$ ), the transition rate of  $\xi(t)$  from  $A_1$  to  $-B_1$  is  $p_1$ , and the inverse transition rate is  $q_1$ .  $\eta(t)$  takes two values  $A_2$  and  $-B_2$  ( $A_2, B_2 > 0$ ), the transition rate of  $\eta(t)$  from  $A_2$  to  $-B_2$  is  $p_2$ , and the inverse transition rate is  $q_2$ . Letting  $\Lambda_\xi$  and  $\Lambda_\eta$  denote the asymmetry of  $\xi(t)$  and  $\eta(t)$ , respectively, we have

$$\begin{aligned} \lambda_\xi &= p_1 + q_1, \sigma_\xi = A_1 B_1, \Lambda_\xi = A_1 - B_1; \\ \lambda_\eta &= p_2 + q_2, \sigma_\eta = A_2 B_2, \Lambda_\eta = A_2 - B_2. \end{aligned}$$

We model both  $\xi(t)$  and  $\eta(t)$  as DN. It is both basic noise and a common colored noise that exists in such materials and devices as metal, transistors, superconducting thin films, and nano-devices. DN also follows the pattern of a Poisson process and is the limiting case (with a correlation rate  $\lambda \rightarrow +\infty$ ) of white Gaussian noise. In addition, the linear differential equation with DN is solvable and thus applicable to a variety of problems [30,31].

In Eq. (6) the external periodic force is a periodically modulated noise. Periodically modulated noise is common in such real-world networks as optical systems and communication systems [12,32,33] in which the external noise  $\eta(t)$  and the periodic input signal  $A \cos(\Omega t)$  interact multiplicatively. Fig. 1 shows a plot of the curves of  $\cos(0.3t) \eta(t)$  in time and frequency domains, and we see that periodically modulated noise  $A \cos(\Omega t) \eta(t)$  varies periodically with time and that the frequency of the periodic input signal  $A \cos(\Omega t)$  characterizes the frequency of the periodically modulated noise.

### 3. The first moment and the amplitude of the output signal

Taking the average of Eq. (6), we obtain

$$\mathcal{D}^\alpha \langle x(t) \rangle + \gamma \mathcal{D}^\beta \langle x(t) \rangle + \omega^2 \langle x(t) \rangle + a_1 \langle \xi(t) x(t) \rangle + a_2 \langle \xi^2(t) x(t) \rangle = 0. \tag{7}$$

Applying the property of the DN yields

$$\langle \xi^2(t) x(t) \rangle = \Lambda_\xi \langle \xi(t) x(t) \rangle + \sigma_\xi \langle x(t) \rangle. \tag{8}$$

Inserting Eq. (8) into Eq. (7) we have

$$\mathcal{D}^\alpha \langle x(t) \rangle + \gamma \mathcal{D}^\beta \langle x(t) \rangle + (\omega^2 + a_2 \sigma_\xi) \langle x(t) \rangle + (a_1 + a_2 \Lambda_\xi) \langle \xi(t) x(t) \rangle = 0. \tag{9}$$

Multiplying Eq. (6) by  $\xi(t)$  and averaging we have

$$\langle \xi(t) \mathcal{D}^\alpha x(t) \rangle + \gamma \langle \xi(t) \mathcal{D}^\beta x(t) \rangle + \omega^2 \langle \xi(t) x(t) \rangle + a_1 \langle \xi^2(t) x(t) \rangle + a_2 \langle \xi^3(t) x(t) \rangle = A \cos(\Omega t) \langle \xi(t) \eta(t) \rangle. \tag{10}$$

Applying the fractional Shapiro–Loginov formula and the property of the DN yields

$$\begin{aligned} \langle \xi(t) \mathcal{D}^\rho x(t) \rangle &= e^{-\lambda_\xi t} \mathcal{D}^\rho (\langle \xi(t) x(t) \rangle e^{\lambda_\xi t}), (0 < \rho \leq 2); \\ \langle \xi^3(t) x(t) \rangle &= (\sigma_\xi + \Lambda_\xi^2) \langle \xi(t) x(t) \rangle + \sigma_\xi \Lambda_\xi \langle x(t) \rangle. \end{aligned} \tag{11}$$

Inserting Eqs. (8) and (11) into Eq. (10) we have

$$\begin{aligned}
 & e^{-\lambda_\xi t} \mathcal{D}^\alpha(\langle \xi(t)x(t) \rangle e^{\lambda_\xi t}) + \gamma e^{-\lambda_\xi t} \mathcal{D}^\beta(\langle \xi(t)x(t) \rangle e^{\lambda_\xi t}) \\
 & + (\omega^2 + a_1 \Lambda_\xi + a_2 \sigma_\xi + a_2 \Lambda_\xi^2) \langle \xi(t)x(t) \rangle + (a_1 \sigma_\xi + a_2 \sigma_\xi \Lambda_\xi) \langle x(t) \rangle \\
 & = \sigma_{\xi\eta} A \cos(\Omega t).
 \end{aligned}
 \tag{12}$$

Letting  $\langle x(t) \rangle = x_1$ ,  $\langle \xi(t)x(t) \rangle = x_2$ , Eqs. (9) and (12) can be written

$$\begin{cases}
 \mathcal{D}^\alpha x_1 + \gamma \mathcal{D}^\beta x_1 + (\omega^2 + a_2 \sigma_\xi) x_1 + (a_1 + a_2 \Lambda_\xi) x_2 = 0, \\
 e^{-\lambda_\xi t} \mathcal{D}^\alpha(x_2 e^{\lambda_\xi t}) + \gamma e^{-\lambda_\xi t} \mathcal{D}^\beta(x_2 e^{\lambda_\xi t}) + (\omega^2 + a_1 \Lambda_\xi + a_2 \sigma_\xi + a_2 \Lambda_\xi^2) x_2 \\
 + (a_1 \sigma_\xi + a_2 \sigma_\xi \Lambda_\xi) x_1 = \sigma_{\xi\eta} A \cos(\Omega t).
 \end{cases}
 \tag{13}$$

To solve Eq. (13) we use the Laplace transform and obtain

$$\begin{cases}
 (s^\alpha + \gamma s^\beta + \omega^2 + a_2 \sigma_\xi) X_1(s) + (a_1 + a_2 \Lambda_\xi) X_2(s) \\
 = (s^{\alpha-1} + \gamma s^{\beta-1}) x_1(0) + s^{\alpha-2} \dot{x}_1(0), \\
 (a_1 \sigma_\xi + a_2 \sigma_\xi \Lambda_\xi) X_1(s) \\
 + [(s + \lambda_\xi)^\alpha + \gamma (s + \lambda_\xi)^\beta + \omega^2 + a_1 \Lambda_\xi + a_2 \sigma_\xi + a_2 \Lambda_\xi^2] X_2(s) \\
 = \sigma_{\xi\eta} \frac{As}{s^2 + \Omega^2} + [(s + \lambda_\xi)^{\alpha-1} + \gamma (s + \lambda_\xi)^{\beta-1}] x_2(0) + (s + \lambda_\xi)^{\alpha-2} \dot{x}_2(0).
 \end{cases}
 \tag{14}$$

where  $X_i(s) = \int_0^{+\infty} x_i(t) e^{-st} dt$ ,  $i = 1, 2$  and  $x_1(0)$ ,  $x_2(0)$ ,  $\dot{x}_1(0)$ ,  $\dot{x}_2(0)$  are the initial conditions.

Letting  $x_3(0) = \dot{x}_1(0)$ ,  $x_4(0) = \dot{x}_2(0)$  solve Eq. (14),  $X_1(s)$  is

$$X_1(s) = H(s) \frac{s}{s^2 + \Omega^2} + H_1(s)x_1(0) + H_2(s)x_2(0) + H_3(s)x_3(0) + H_4(s)x_4(0),
 \tag{15}$$

with

$$\begin{aligned}
 H(s) &= \frac{-\sigma_{\xi\eta} A d_{12}}{d_{11} d_{22} - d_{12} d_{21}}, \\
 H_1(s) &= \frac{d_{22}(s^{\alpha-1} + \gamma s^{\beta-1})}{d_{11} d_{22} - d_{12} d_{21}}, \\
 H_2(s) &= -\frac{d_{12} [(s + \lambda_\xi)^{\alpha-1} + \gamma (s + \lambda_\xi)^{\beta-1}]}{d_{11} d_{22} - d_{12} d_{21}}, \\
 H_3(s) &= \frac{d_{22} s^{\alpha-2}}{d_{11} d_{22} - d_{12} d_{21}}, \\
 H_4(s) &= -\frac{d_{12} (s + \lambda_\xi)^{\alpha-2}}{d_{11} d_{22} - d_{12} d_{21}}, \\
 d_{11} &= s^\alpha + \gamma s^\beta + \omega^2 + a_2 \sigma_\xi, \\
 d_{12} &= a_1 + a_2 \Lambda_\xi, \\
 d_{13} &= (s^{\alpha-1} + \gamma s^{\beta-1}) x_1(0) + s^{\alpha-2} \dot{x}_1(0), \\
 d_{21} &= a_1 \sigma_\xi + a_2 \sigma_\xi \Lambda_\xi, \\
 d_{22} &= (s + \lambda_\xi)^\alpha + \gamma (s + \lambda_\xi)^\beta + \omega^2 + a_1 \Lambda_\xi + a_2 \sigma_\xi + a_2 \Lambda_\xi^2, \\
 d_{23} &= [(s + \lambda_\xi)^{\alpha-1} + \gamma (s + \lambda_\xi)^{\beta-1}] x_2(0) + (s + \lambda_\xi)^{\alpha-2} \dot{x}_2(0).
 \end{aligned}$$

Using the inverse Laplace transform on Eq. (15) we obtain the solution of the first moment

$$\langle x(t) \rangle = x_1(t) = \int_0^t h(t - \tau) \cos(\Omega \tau) d\tau + \sum_{k=1}^4 h_k(t) x_k(0),
 \tag{16}$$

where the Laplace transform of  $h(t)$  and  $h_k(t)$ , ( $k = 1, 2, 3, 4$ ) are  $H(s)$  and  $H_k(s)$ , ( $k = 1, 2, 3, 4$ ) respectively.

In the long time limit  $t \rightarrow +\infty$  the influence of the initial conditions disappears and the long time behavior of the first moment from Eq. (16) is

$$\langle x(t) \rangle_{as} = \langle x(t) \rangle_{t \rightarrow +\infty} = \int_0^t h(t - \tau) \cos(\Omega \tau) d\tau = A_{st} \cos(\Omega t + \varphi),
 \tag{17}$$

where  $A_{st}$  and  $\varphi$  are the amplitude and the phase shift of  $\langle x(t) \rangle_{as}$ , respectively.

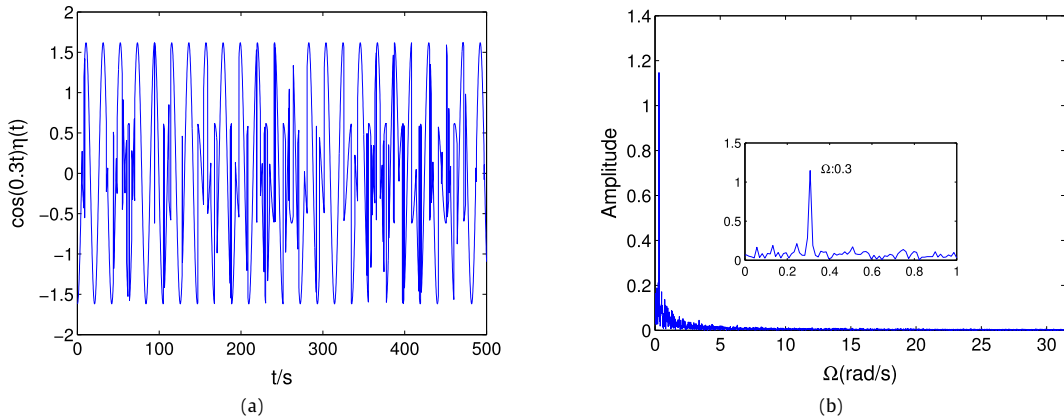


**Fig. 1.** (color online) The periodically modulated noise  $\cos(0.3t)\eta(t)$ : (a) time domain; (b) frequency domain. Other parameter values:  $\lambda_\eta = 0.5, \sigma_\eta = 1, \Lambda_\eta = 1$ .

Using Eq. (15) we obtain the amplitude and the phase shift,

$$\begin{cases} A_{st} = \frac{A\sigma_\xi\eta|d_{12}|}{\sqrt{f_1^2 + f_2^2}}, \\ \varphi = -\arctan\left(\frac{f_2}{f_1}\right), \end{cases} \tag{18}$$

where

$$\begin{aligned} f_1 = & \Omega^\alpha k^\alpha \cos\left(\frac{\pi}{2}\alpha + \theta\alpha\right) + \gamma\Omega^\alpha k^\beta \cos\left(\frac{\pi}{2}\alpha + \theta\beta\right) \\ & + (\omega^2 + a_1\Lambda_\xi + a_2\sigma_\xi + a_2\Lambda_\xi^2)\Omega^\alpha \cos\left(\frac{\pi}{2}\alpha\right) + \gamma\Omega^\beta k^\alpha \cos\left(\frac{\pi}{2}\beta + \theta\alpha\right) \\ & + \gamma^2\Omega^\beta k^\beta \cos\left(\frac{\pi}{2}\beta + \theta\beta\right) + (\omega^2 + a_1\Lambda_\xi + a_2\sigma_\xi + a_2\Lambda_\xi^2)\gamma\Omega^\beta \cos\left(\frac{\pi}{2}\beta\right) \\ & + k^\alpha(\omega^2 + a_2\sigma_\xi)\cos(\theta\alpha) + \gamma k^\beta(\omega^2 + a_2\sigma_\xi)\cos(\theta\beta) \\ & + (\omega^2 + a_2\sigma_\xi)(\omega^2 + a_1\Lambda_\xi + a_2\sigma_\xi + a_2\Lambda_\xi^2) - d_{12}d_{21}, \end{aligned}$$

$$\begin{aligned} f_2 = & \Omega^\alpha k^\alpha \sin\left(\frac{\pi}{2}\alpha + \theta\alpha\right) + \gamma\Omega^\alpha k^\beta \sin\left(\frac{\pi}{2}\alpha + \theta\beta\right) \\ & + (\omega^2 + a_1\Lambda_\xi + a_2\sigma_\xi + a_2\Lambda_\xi^2)\Omega^\alpha \sin\left(\frac{\pi}{2}\alpha\right) + \gamma\Omega^\beta k^\alpha \sin\left(\frac{\pi}{2}\beta + \theta\alpha\right) \\ & + \gamma^2\Omega^\beta k^\beta \sin\left(\frac{\pi}{2}\beta + \theta\beta\right) + (\omega^2 + a_1\Lambda_\xi + a_2\sigma_\xi + a_2\Lambda_\xi^2)\gamma\Omega^\beta \sin\left(\frac{\pi}{2}\beta\right) \\ & + k^\alpha(\omega^2 + a_2\sigma_\xi)\sin(\theta\alpha) + \gamma k^\beta(\omega^2 + a_2\sigma_\xi)\sin(\theta\beta), \end{aligned}$$

$$k = \sqrt{\lambda_\xi^2 + \Omega^2},$$

$$\theta = \arctan\left(\frac{\Omega}{\lambda_\xi}\right).$$

#### 4. The resonant behavior of the output amplitude

Note that from Eq. (18) the behavior of the output amplitude  $A_{st}$  is fully determined by the combined system parameters  $\alpha, \beta, \omega, \gamma, a_1, a_2, \sigma_\xi, \lambda_\xi, \sigma_{\xi\eta}$ , and  $\Omega$ . We next examine the effect of nonlinear noise and fractional-order damping on the output amplitude.

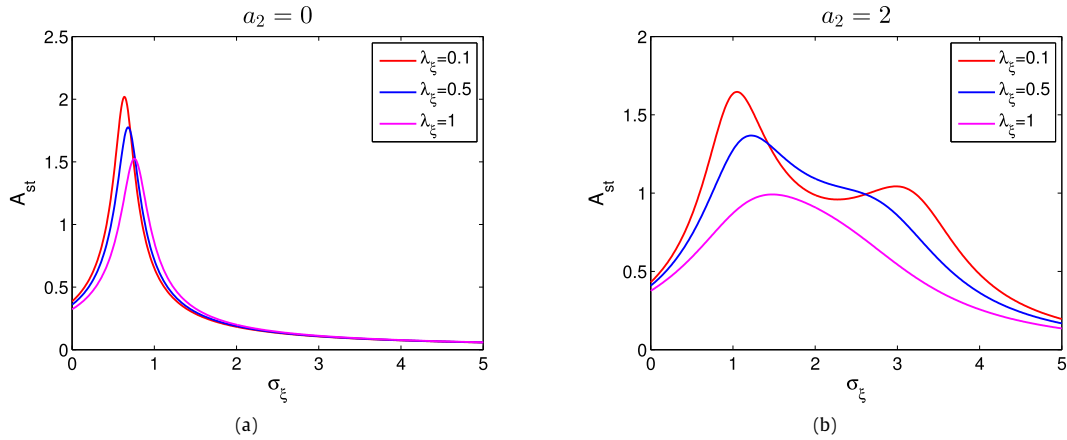


**Fig. 2.** (color online) The output amplitude  $A_{st}$  versus noise intensity  $\sigma_\xi$  with various  $\lambda_\xi$ : (a)  $a_2 = 0$ ; (b)  $a_2 = 2$ . Other parameter values:  $\gamma = 1, \alpha = 1.5, \beta = 0.1, \omega = 1, a_1 = 4, A_\xi = 1, \sigma_{\xi\eta} = 1, \Omega = 0.3, A = 1$ .

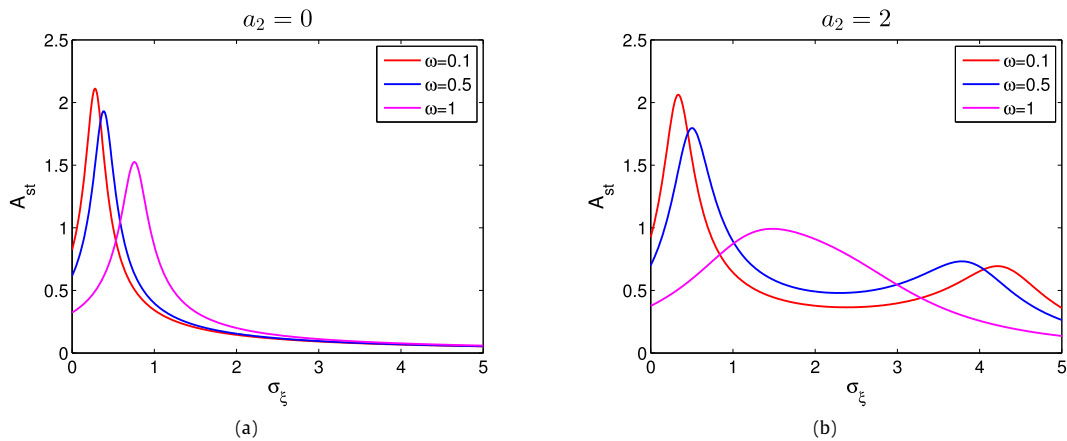


**Fig. 3.** (color online) The output amplitude  $A_{st}$  versus noise intensity  $\sigma_\xi$  with various  $\omega$ : (a)  $a_2 = 0$ ; (b)  $a_2 = 2$ . Other parameter values:  $\gamma = 1, \alpha = 1.5, \beta = 0.1, a_1 = 4, A_\xi = 1, \lambda_\xi = 1, \sigma_{\xi\eta} = 1, \Omega = 0.3, A = 1$ .

4.1. The effect of nonlinear noise on the output amplitude  $A_{st}$

Figs. 2–6 plot the curves of  $A_{st}$  as a function of  $\sigma_\xi$  with different parameter values, including  $a_1, \lambda_\xi, \Omega, \omega,$  and  $\beta$ . To study the effect of nonlinear noise on the output amplitude, we consider two situations, (i)  $a_2 = 0$  in which the system is driven by linear noise, and (ii)  $a_2 = 2$  in which the system is driven by quadratic noise. Figs. 2a–6a show that when the system is driven by linear noise (i.e.,  $a_2 = 0$ ) all the curves of  $A_{st}(\sigma_\xi)$  show a resonance with one peak, and the position and height of the resonance peaks are dependent on the parameters  $a_1, \lambda_\xi, \Omega, \omega,$  and  $\beta$ . Figs. 2b–6b show that when the system is driven by a quadratic noise (i.e.,  $a_2 = 2$ ) the evolution of  $A_{st}$  versus  $\sigma_\xi$  shows two resonant behaviors: resonance with one peak and multiresonance with two peaks. This resonant behavior is determined by a combination of  $a_2, a_1, \lambda_\xi, \Omega, \omega,$  and  $\beta$ .

Thus the effect of nonlinear noise on the output amplitude differs from that of linear noise. When the system is driven by nonlinear noise, the evolution of  $A_{st}$  versus  $\sigma_\xi$  exhibits a more resonant behavior. This is because when the intrinsic frequency of the system is affected by nonlinear noise  $a_1\xi(t) + a_2\xi^2(t)$  the potential

$$U(x, t) = [\omega^2 + a_1\xi(t) + a_2\xi^2(t)]x^2(t)/2$$

is strongly dependent on the nature of  $\xi(t)$  and the way in which nonlinear noise is generated, thus the fluctuation of potential is more complex. The SR phenomenon is a nonlinear cooperative effect jointly induced by external driving, noise and the system. The resonant behavior of  $A_{st}(\sigma_\xi)$  is changed under the combined action of complex fluctuating potential, systemic, and external periodic forces.

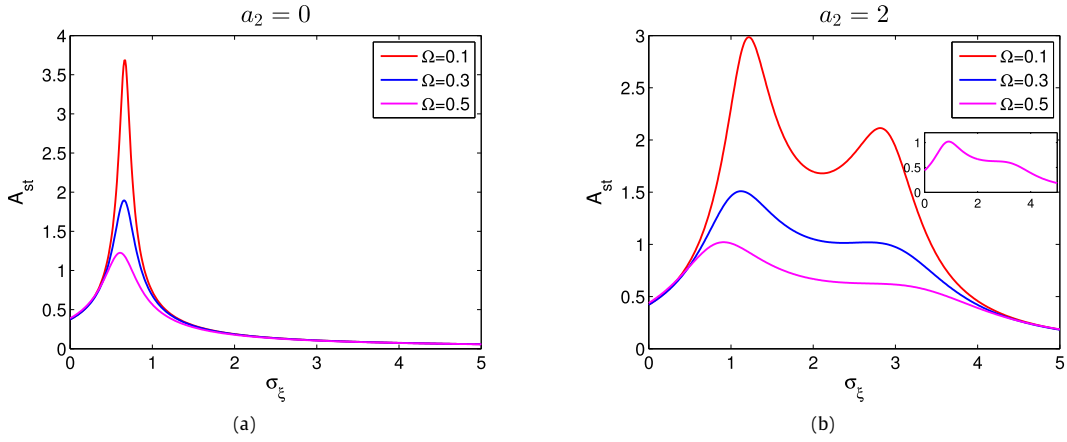


**Fig. 4.** (color online) The output amplitude  $A_{st}$  versus noise intensity  $\sigma_\xi$  with various  $\Omega$ : (a)  $a_2 = 0$ ; (b)  $a_2 = 2$ . Other parameter values:  $\gamma = 1, \omega = 1, \alpha = 1.5, \beta = 0.1, a_1 = 4, \Lambda_\xi = 1, \lambda_\xi = 0.3, \sigma_{\xi\eta} = 1, A = 1$ .

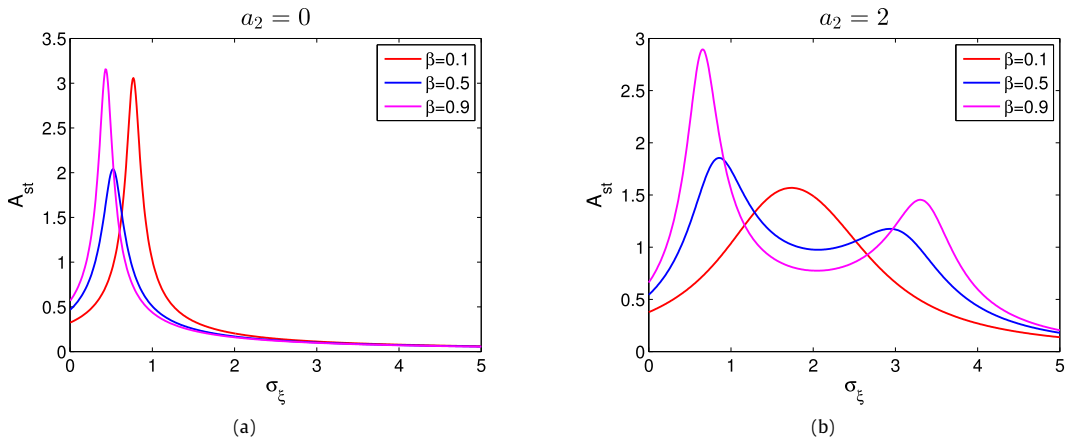


**Fig. 5.** (color online) The output amplitude  $A_{st}$  versus noise intensity  $\sigma_\xi$  with various  $\beta$ : (a)  $a_2 = 0$ ; (b)  $a_2 = 2$ . Other parameter values:  $\gamma = 1, \omega = 1, \alpha = 1.5, a_1 = 4, \Lambda_\xi = 1, \lambda_\xi = 1, \sigma_{\xi\eta} = 1, \Omega = 0.1, A = 1$ .

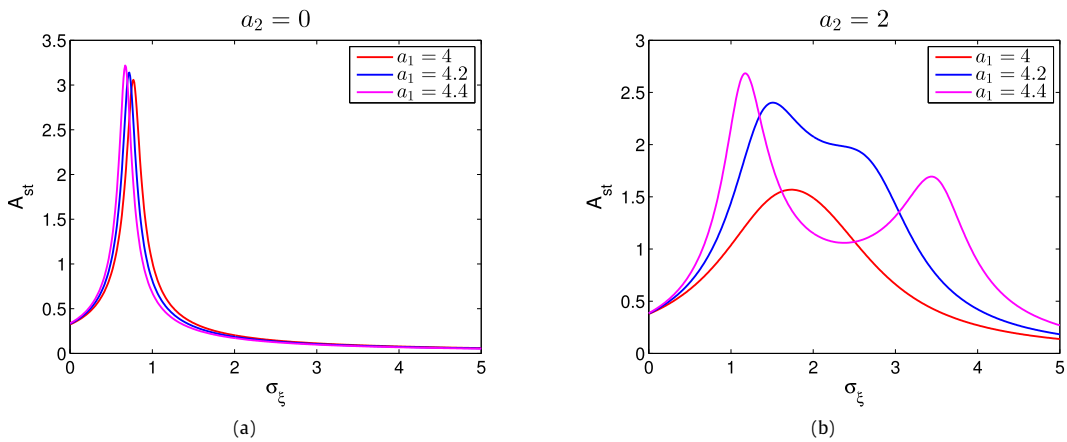


**Fig. 6.** (color online) The output amplitude  $A_{st}$  versus noise intensity  $\sigma_\xi$  with various  $a_1$ : (a)  $a_2 = 0$ ; (b)  $a_2 = 2$ . Other parameter values:  $\gamma = 1, \omega = 1, \alpha = 1.5, \beta = 0.1, \Lambda_\xi = 1, \lambda_\xi = 1, \sigma_{\xi\eta} = 1, \Omega = 0.1, A = 1$ .

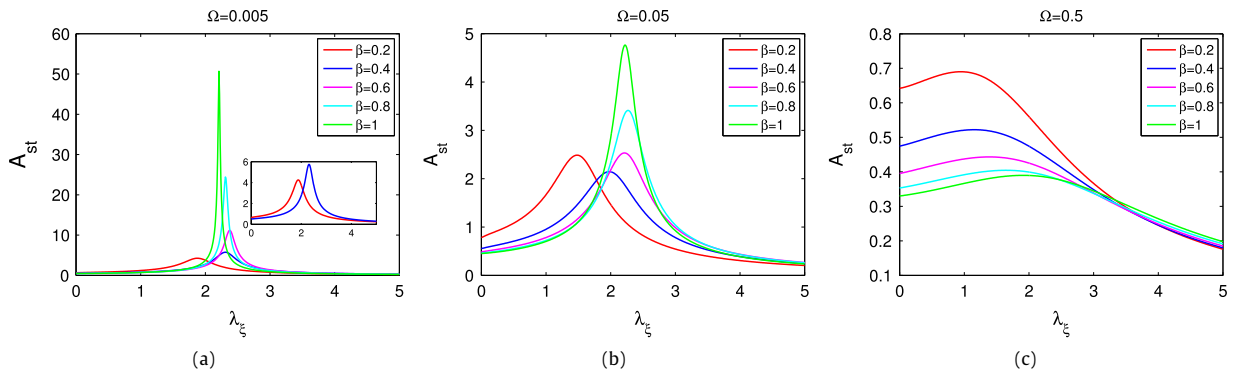


**Fig. 7.** (color online) The output amplitude  $A_{st}$  versus noise correlation rate  $\lambda_\xi$  with various  $\beta$ : (a)  $\Omega = 0.005$ ; (b)  $\Omega = 0.05$ ; (c)  $\Omega = 0.5$ . Other parameter values:  $\gamma = 1$ ,  $\omega = 1$ ,  $\alpha = 1.5$ ,  $a_1 = 4$ ,  $a_2 = 1$ ,  $\Lambda_\xi = 1$ ,  $\sigma_{\xi\eta} = 1$ ,  $\sigma_\xi = 1$ ,  $A = 1$ .

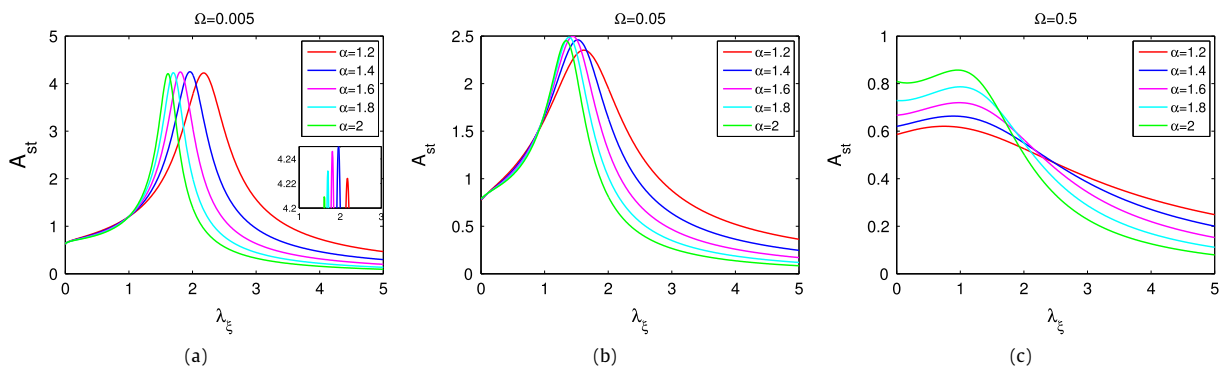


**Fig. 8.** (color online) The output amplitude  $A_{st}$  versus noise correlation rate  $\lambda_\xi$  with various  $\alpha$ : (a)  $\Omega = 0.005$ ; (b)  $\Omega = 0.05$ ; (c)  $\Omega = 0.5$ . Other parameter values:  $\gamma = 1$ ,  $\omega = 1$ ,  $\beta = 0.2$ ,  $a_1 = 4$ ,  $a_2 = 1$ ,  $\Lambda_\xi = 1$ ,  $\sigma_{\xi\eta} = 1$ ,  $\sigma_\xi = 1$ ,  $A = 1$ .

#### 4.2. The effect of the fractional-order damping on output amplitude $A_{st}$

Here we study the effect of fractional-order external damping and fractional-order intrinsic damping on the system. Fig. 7 shows curves of  $A_{st}$  as a function of  $\lambda_\xi$  with different  $\beta$  and  $\Omega$  values. Fig. 7a shows that the frequency of the external periodic force is  $\Omega = 0.005$ . The partial enlarged drawing shows the curves of  $A_{st}(\lambda_\xi)$  for  $\beta = 0.2$  and  $\beta = 0.4$ . We see that the curves of  $A_{st}(\lambda_\xi)$  have a resonance with one peak, and that as the value of  $\beta$  increases the resonance peak increases, with its position first moving toward the right and then toward the left. This means that increasing  $\beta$  enhances the resonance for  $\Omega = 0.005$ . Fig. 7b shows that the frequency of the external periodic force is  $\Omega = 0.05$ , that the curves of  $A_{st}(\lambda_\xi)$  have a resonance with one peak, that as the value of  $\beta$  increases the resonance peak first becomes lower and then higher, and that the position of the peak first moves toward the right and then toward the left. Increasing of  $\beta$  thus first suppresses and then enhances the resonance for  $\Omega = 0.05$ . Fig. 7c shows that the frequency of the external periodic force is  $\Omega = 0.5$ , that the curves of  $A_{st}(\lambda_\xi)$  display a resonance with one peak, and that as the value of  $\beta$  increases the resonance peak becomes lower. This means increasing  $\beta$  suppresses the resonance for  $\Omega = 0.5$ .

Fig. 8 shows the curves of  $A_{st}(\lambda_\xi)$  for different  $\alpha$  and  $\Omega$  values. Figs. 8a and 8b show that the frequencies of the external periodic force are  $\Omega = 0.005$  and  $\Omega = 0.05$ , respectively, that the curves of  $A_{st}(\lambda_\xi)$  have a resonance with one peak, that as the value of  $\alpha$  increases the resonance peak first becomes higher and then becomes lower, and that the position of the peak moves toward the left. This means the increasing of  $\alpha$  first enhances and then suppresses the resonance for  $\Omega = 0.005$  and  $\Omega = 0.05$ . Fig. 8c shows that the frequency of the external periodic force is  $\Omega = 0.5$ , that the curves of  $A_{st}(\lambda_\xi)$  display a resonance with one peak, and that as the value of  $\alpha$  increases the resonance peak becomes higher. This means increasing  $\alpha$  enhances the resonance for  $\Omega = 0.5$ .

Figs. 7 and 8 show that the order of the fractional-order damping strongly affects resonant intensity. When the external periodic force is high-frequency, the higher the order of fractional-order intrinsic damping, the higher will be the resonant intensity, and the higher the order of fractional-order external damping, the smaller will be the resonant intensity. This can be due to the amplitude frequency characteristic of the fractional calculus. The fractional-order damping term  $\mathcal{D}^\rho x(t)$  is the Caputo's fractional derivative of  $x(t)$ . The integral and derivative are inverse operations to each other, and an acting

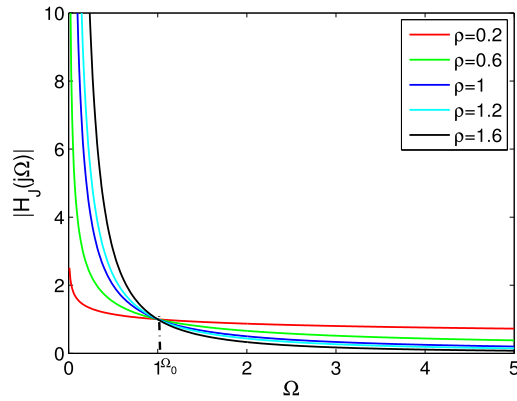


Fig. 9. (color online) Amplitude frequency characteristics of fractional integral.

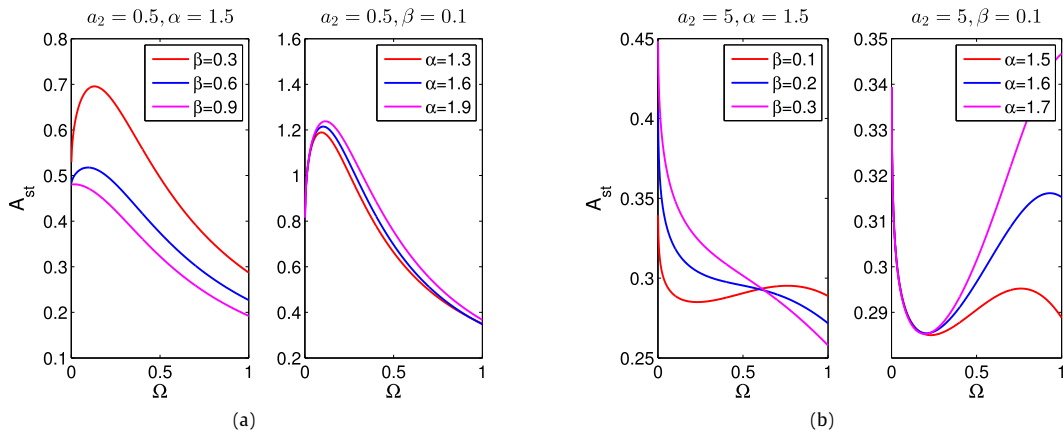


Fig. 10. (color online) The output amplitude  $A_{st}$  versus the frequency  $\Omega$  of the external periodic force with various  $\alpha, \beta$ : (a)  $a_2 = 0.5$ ; (b)  $a_2 = 5$ . Other parameter values:  $\gamma = 1, \omega = 1, a_1 = 4.2, \Lambda_\xi = 1, \lambda_\xi = 1, \sigma_{\xi\eta} = 1, \sigma_\xi = 1, A = 1$ .

fractional derivative on the output signal  $x(t)$  implies an acting fractional integral on the input signal  $f(t)$ . The Caputo's fractional integral of  $f(t)$  is defined [34]

$$\mathcal{J}^\rho f(t) = \int_0^t \frac{(t - \tau)^{\rho-1}}{\Gamma(\rho)} f(\tau) d\tau = \frac{t^{\rho-1}}{\Gamma(\rho)} * f(t), (\rho > 0),$$

where  $*$  is the convolution. The amplitude frequency characteristic of fractional integral is  $|H_{\mathcal{J}}(j\Omega)| = \Omega^{-\rho}$  and the variation curves of  $|H_{\mathcal{J}}(j\Omega)|$  is shown in Fig. 9. This figure shows that the gain of the fractional integral has a power-law decrease as the frequency increases, and that when  $\Omega < \Omega_0$  the larger the order of  $\rho$ , the larger will be the gain. When  $\Omega > \Omega_0$ , the larger the order  $\rho$ , the smaller will be the gain. This confirms that the resonant intensity is related to the orders  $\alpha, \beta$  of fractional-order damping and the frequency  $\Omega$  of the external periodic force. These results can be also explained from a physical point of view. When the Brownian particle is driven by external periodic force in the viscoelastic media, its periodic motion is closely related with the external damping force and itself energy consumption. Therefore the resonant intensity is connected to the orders  $\alpha, \beta$  of fractional-order damping. In addition, the behavior of the system with double fractional-order derivatives differs from the system with a single fractional-order derivative.

Because the resonant intensity is associated with  $\alpha, \beta$ , and  $\Omega$ , the evolution of output amplitude  $A_{st}$  versus  $\Omega$  exhibits various resonant behaviors shown in Fig. 10.

Fig. 10 shows the curves of  $A_{st}(\Omega)$  for different  $a_2, \alpha$ , and  $\beta$  values. Fig. 10a shows that the quadratic coefficient of noise is  $a_2 = 0.5$ , that the curves of  $A_{st}(\Omega)$  display resonance with one peak, and that the resonant behavior does not change with  $\alpha$  and  $\beta$ . Fig. 10b shows that the quadratic coefficient of noise is  $a_2 = 5$ , that the curves of  $A_{st}(\Omega)$  display resonance with one peak and one valley and with one valley, and that the resonant behavior is closely related to  $\alpha$  and  $\beta$ .

Fig. 10 shows that the output amplitude  $A_{st}(\Omega)$  exhibits three resonant behaviors: resonance with one peak, resonance with one peak and one valley, and resonance with one valley. The resonant behavior is closely linked to the nonlinear term of nonlinear noise and to the orders  $\alpha, \beta$  of the fractional-order damping.

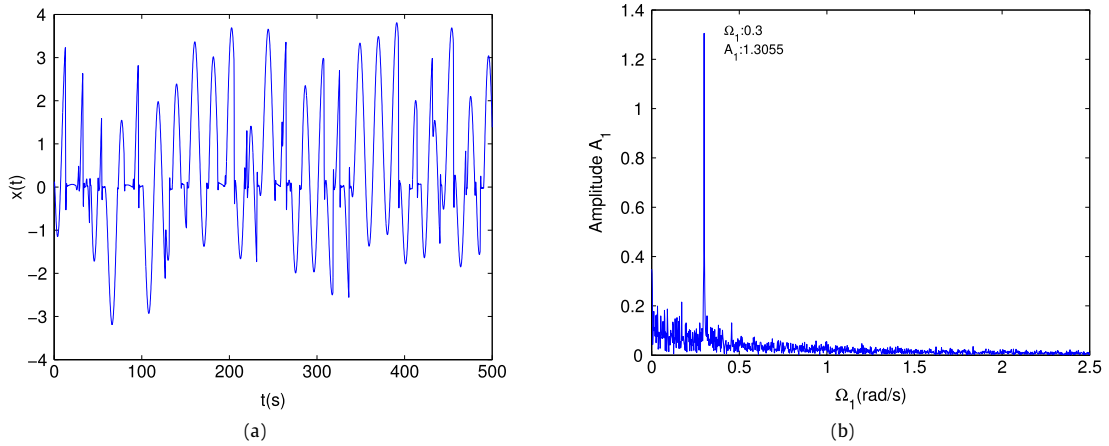


Fig. 11. (color online) The output signal 1 for Eq. (6): (a) time domain; (b) frequency domain.

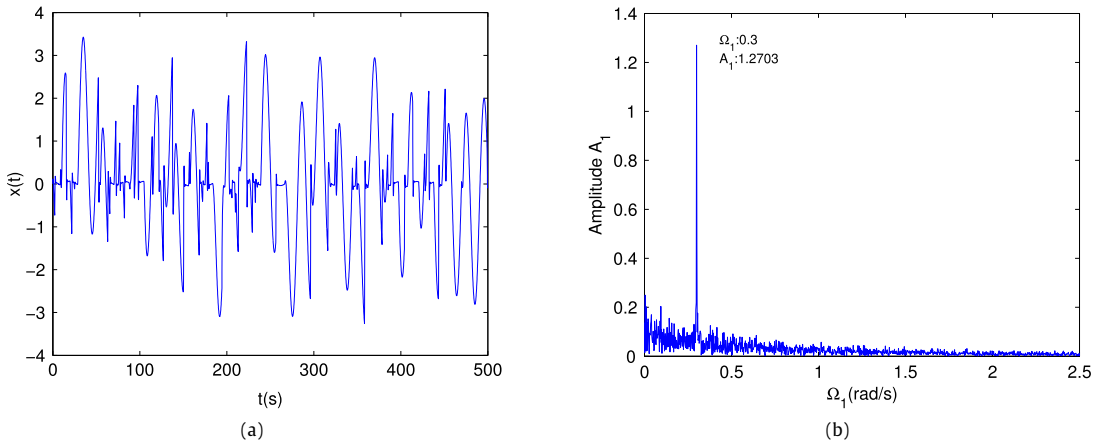


Fig. 12. (color online) The output signal 2 for Eq. (6): (a) time domain; (b) frequency domain.

The mechanism for the SR phenomena in Fig. 10 can be explained as follows. The characteristic of the fluctuating potential

$$U(x, t) = [\omega^2 + a_1\xi(t) + a_2\xi^2(t)]x^2(t)/2$$

is closely related to nonlinear noise  $a_1\xi(t) + a_2\xi^2(t)$ . At the same time the impact of  $\alpha$  and  $\beta$  on the resonant behavior strongly depends on  $\Omega$  (see Figs. 7–9). Thus there are various SR phenomena under the combined action of nonlinear noise, fractional-order external damping, and fractional-order intrinsic damping. Note that the SR phenomena in Fig. 10 agree with those in Figs. 7–8.

### 5. Numerical simulations

We now use numerical simulations to verify the accuracy of the analytic results. We use the predictor–corrector approach [35,36] to obtain a numerical solution for Eq. (6). Figs. 11 and 12 show two different output signals for Eq. (6) under the same simulation conditions. The simulation time and time step affect the speed and accuracy of computation in numerical simulation. In general, the larger time step should be selected without decreasing computational accuracy. In this paper, the simulation time is  $T = 3000$  s, the time step  $T_s = 0.1$  s, the multiplicative noise intensity  $\sigma_\xi = 1$ , the multiplicative noise correlation rate  $\lambda_\xi = 0.5$ , and the values of other parameters the same as those in Fig. 2b.

When the oscillator is driven by nonlinear noise  $4\xi(t) + 2\xi^2(t)$  and the external periodic force  $\cos(0.3t)\eta(t)$ . Figs. 11b and 12b show that output signal 1 and output signal 2 present a spike at  $\Omega_1 = 0.3$  in the frequency domain, respectively. Thus the system output signal is a simple harmonic vibration that has the same frequency as the external periodic force. We also find that the value of output amplitude in Fig. 11b is  $A_1(\Omega_1 = 0.3) = 1.3055$ , and the value of output amplitude

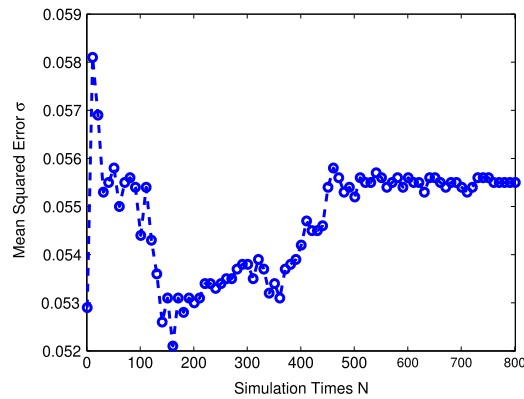


Fig. 13. (color online) The mean squared error  $\sigma$  versus the simulation times  $N$ .

in Fig. 12b is  $A_1(\Omega_1 = 0.3) = 1.2703$ . Within the allowable error, the numerical simulation results  $A_1 = 1.3055$  and  $A_1 = 1.2703$  agree with the analytical result  $A_{st} = 1.2748$  given by Eq. (18).

Under the same simulation conditions, the discrepancy in the simulation results occurs because the output amplitude is a random variable in the presence of noise. To take the influence of noise into consideration, we use the Monte-Carlo method to obtain the mean squared error (MSE)  $\sigma$  versus simulation times  $N$ , where  $\sigma = \sqrt{\frac{1}{N} \sum_{n=1}^N (A_{1n} - A_{st})^2}$ ,  $A_{1n}$ ,  $n = 1, 2, \dots, N$  is the simulation  $n$  result given by the numerical simulation, and  $A_{st}$  is the analytical result obtained by Eq. (18). Fig. 13 shows the behavior of the mean squared error  $\sigma$  as a function of simulation times  $N$ , where the values of parameters are the same as those in Figs. 11 and 12. Fig. 13 shows that the mean squared error gradually stabilizes ( $\sigma \rightarrow 5.55 \times 10^{-2}$ ) when the simulation time  $N$  is large enough ( $N > 500$ ). Thus the numerical simulation result agrees with the analytical result given by Eq. (18).

## 6. Conclusions

We have considered an oscillator with fractional-order external damping and fractional-order intrinsic damping driven by the quadratic noise, which is the most basic nonlinear noise. In our proposed model, we obtain an analytical expression of the output amplitude and find various non-monotonic behaviors in the output amplitude. In particular, we focus on the impact of nonlinear noise, fractional-order external damping, and fractional-order intrinsic damping on the resonant behavior. We also present numerical simulations to verify the accuracy of the analytic results and demonstrate reliability of our findings and their value in practical applications. Our conclusions are as follows:

- (1) The system output response is a simple harmonic vibration that has the same frequency as the external periodic force. The nonlinear noise plays a key role in system behavior. In quadratic noise the evolution of output amplitude versus multiplicative noise intensity exhibits a more resonant behavior. There is resonance with one peak and multiresonance with two peaks. The resonant behavior is determined by the combination of  $a_2$ ,  $a_1$ ,  $\lambda_\xi$ ,  $\Omega$ ,  $\omega$ , and  $\beta$  values.
- (2) The order of the fractional-order damping strongly impacts resonant intensity. The impact of the order of fractional-order external damping on the resonant intensity is opposite to the impact of the order of fractional-order intrinsic damping. When the external periodic force is high-frequency, the higher the order of fractional-order intrinsic damping, the bigger will be the resonant intensity, and the higher the order of fractional-order external damping, the smaller will be the resonant intensity.
- (3) The evolution of the output amplitude versus the frequency of the external periodic force exhibits three behaviors: a resonance with one peak, a resonance with one peak and one valley, and a resonance with one valley.

In conclusion, the research shows that the nonlinearity of nonlinear noise plays a key role in resonant behavior, and that a system with double fractional-order derivatives generates a more complex resonance effect than a system with a single fractional-order derivative. Under the combined action of nonlinear noise, fractional-order external damping, and fractional-order intrinsic damping the system presents an abundance of resonant behaviors. The results we present here provide a theoretical foundation for further research on the effect of nonlinear noise on dynamic behaviors, and will be valuable to those developing practical applications.

## Acknowledgments

This work was supported by the National Natural Science Foundation of P.R. China (Grant Nos. 11526172, 11501385, 11601450), the Scientific Research Foundation of SWPU (Grant Nos. 2013XJZ027, 2013XJZ025, 2014PYZ015).

## References

- [1] R. Hilfer, *Applications of Fractional Calculus in Physics*, World Scientific, Singapore, 2000, p. i.
- [2] A. Tofghi, The intrinsic damping of the fractional oscillator, *Physica A* 329 (2003) 29–34.
- [3] Y.E. Ryabov, A. Puzenko, Damped oscillations in view of the fractional oscillator equation, *Phys. Rev. B* 66 (2002) 184201.
- [4] B.N.N. Achar, J.W. Hanneken, T. Clarke, Response characteristics of a fractional oscillator, *Physica A* 309 (2002) 275–288.
- [5] K. Wiesenfeld, F. Moss, Stochastic resonance and the benefits of noise: from ice ages to crayfish and SQUIDS, *Nature* 373 (1995) 33–36.
- [6] R. Benzi, A. Sutera, A. Vulpiani, The mechanism of stochastic resonance, *J. Phys. A: Math. Gen.* 14 (1981) L453–L457.
- [7] M. Gitterman, Overdamped harmonic oscillator with multiplicative noise, *Physica A* 352 (2005) 309–334.
- [8] M. Gitterman, I. Shapiro, Stochastic resonance in a harmonic oscillator with random mass subject to asymmetric dichotomous noise, *J. Stat. Phys.* 144 (2011) 139–149.
- [9] Y. Tian, L. Huang, M.K. Luo, Effects of time-periodic modulation of cross-correlation intensity between noises on stochastic resonance of over-damped linear system, *Acta Phys. Sinica* 62 (2013) 050502.
- [10] M. Gitterman, Harmonic oscillator with fluctuating damping parameter, *Phys. Rev. E* 69 (2004) 041101.
- [11] G.T. He, Y. Tian, Y. Wang, Stochastic resonance in a fractional oscillator with random damping strength and random spring stiffness, *J. Stat. Mech.* 9 (2013) P09026.
- [12] T. Yu, L. Zhang, M.K. Luo, Stochastic resonance in the fractional Langevin equation driven by multiplicative noise and periodically modulated noise, *Phys. Scr.* 88 (2013) 045008.
- [13] L.F. Lin, Y. Tian, H. Ma, Stochastic resonance in an over-damped linear oscillator, *Chin. Phys. B* 23 (2014) 080503.
- [14] T. Yu, M.K. Luo, Y. Hua, The resonant behavior of fractional harmonic oscillator with fluctuating mass, *Acta Phys. Sinica* 62 (2013) 210503.
- [15] E. Soika, R. Mankin, A. Ainsaar, Resonant behavior of a fractional oscillator with fluctuating mass, *Phys. Rev. E* 81 (2010) 011141.
- [16] L.F. Lin, C. Chen, S.C. Zhong, H.Q. Wang, Stochastic resonance in a fractional oscillator with random mass and random frequency, *J. Stat. Phys.* 160 (2015) 497–511.
- [17] S.C. Zhong, H. Ma, H. Peng, L. Zhang, Stochastic resonance in a harmonic oscillator with fractional-order external and intrinsic dampings, *Nonlinear Dynam.* 82 (2015) 535–545.
- [18] X.M. Liang, L. Zhao, Z.H. Liu, Phase-noise-induced resonance in a single neuronal system, *Phys. Rev. E* 84 (2011) 031916.
- [19] A. Ishimaru, *Wave Propagation and Scattering in Random Media*, Academic Press, San Diego, CA, 1978.
- [20] O.M. Phillips, *The Dynamics of the Upper Ocean*, Cambridge University Press, 1977.
- [21] B.J. West, S. Venkita, Model of gravity wave growth due to fluctuations in the air-sea coupling parameter, *J. Geophys. Res.* 86 (1981) 4293–4298.
- [22] A. Couairon, J.M. Chomaz, Fully nonlinear global modes in slowly varying flows, *Phys. Fluids* 11 (1999) 3688–3703.
- [23] F. Heslot, A. Libchaber, Unidirectional crystal growth and crystal anisotropy, *Phys. Scr.* T9 (1985) 126–129.
- [24] M.S. Abdalla, Time-dependent harmonic oscillator with variable mass under the action of a driving force, *Phys. Rev. A* 34 (1987) 4598–4605.
- [25] S. Murray, M.O. Scully, W.E. Lamb, *Laser Physics*, Addison-Wesley Publishing, Red wood city, 1974.
- [26] L.Y. Zhang, L. Cao, D.J. Wu, Stochastic resonance in linear region of a single-mode laser: effects of amplitude modulation of signal, *Commun. Theor. Phys.* 49 (2008) 1310–1314.
- [27] J.M. Sancho, M.S. Miguel, D. Dürr, Adiabatic elimination for systems of Brownian particles with nonconstant damping coefficients, *J. Stat. Phys.* 28 (1982) 291–305.
- [28] F. Sagués, M. San Miguel, J.M. Sancho, Nonmarkovian dynamics of stochastic differential equations with quadratic noise, *Z. Phys. B* 55 (1984) 269–282.
- [29] H. Calisto, F. Mora, E. Tirapegui, Stochastic resonance in a linear system: An exact solution, *Phys. Rev. E* 74 (2006) 022102.
- [30] I. Bena, C.V.D. Broeck, R. Kawai, K. Lindenberg, Nonlinear response with dichotomous noise, *Phys. Rev. E* 66 (2002) 045603.
- [31] I. Bena, Dichotomous Markov noise: Exact results for out-of-equilibrium systems, *Internat. J. Modern Phys. B* 20 (2006) 2825–2888.
- [32] M.I. Dykman, D.G. Luchinsky, P.V. McClintock, N.D. Stein, N.G. Stocks, Stochastic resonance for periodically modulated noise intensity, *Phys. Rev. A* 46 (1992) R1713–R1716.
- [33] J. Wang, L. Cao, D.J. Wu, Stochastic multiresonance for periodically modulated noise in a singlemode laser, *Chin. Phys. Lett.* (20) (2003) 1217–1220.
- [34] I. Podlubny, *Fractional Differential Equations*, Academic Press, San Diego, CA, 1999.
- [35] W.H. Deng, Numerical algorithm for the time fractional Fokker-Planck equation, *J. Comput. Phys.* 227 (2007) 1510–1522.
- [36] W.H. Deng, E. Barkai, Ergodic properties of fractional Brownian-Langevin motion, *Phys. Rev. E* 79 (2009) 011112.